

Cr–CO Photodissociation in Cr(CO)₆: Reassessment of the Role of Ligand-Field Excited States in the Photochemical Dissociation of Metal–Ligand Bonds

C. Pollak,[†] A. Rosa, and E. J. Baerends*

Contribution from the Afdeling Theoretische Chemie, Vrije Universiteit, 1081HV Amsterdam, The Netherlands

Received February 24, 1997[⊗]

Abstract: Density functional calculations have been performed on the excited states of Cr(CO)₆. In contrast to the generally accepted assignment of the spectrum by Gray and Beach^{1,2} but in agreement with recent CASSCF/CASPT2 calculations by Pierloot et al.³ we find the low-intensity absorption at the low-energy side of the first charge-transfer (CT) band not to be due to ligand-field (LF) excited states, but to symmetry forbidden CT excitations. In Cr(CO)₆ as in other d⁶ metal–carbonyl complexes,^{4–6} the LF states are at high energy. The calculations show that two states arising from the low-energy CT configuration have dissociative potential energy surfaces, in agreement with the experimentally observed photodissociation of the Cr–CO bond upon low-energy absorption. The photodissociation is therefore occurring from CT and not from LF states. This leads to a reassessment of the role of LF states in metal–ligand photodissociation: it is not necessary to excite to LF states in order to induce photodissociation of ligands, and such dissociation, when observed, does not prove that the excitation was to a LF state.

1. Introduction

The accepted picture of photochemical dissociation of metal–ligand bonds gives a predominant role to ligand-field excitations.^{7,8} The argument may be illustrated with the well-known qualitative molecular orbital energy diagram for an octahedral d⁶ transition-metal complex depicted in Figure 1. In this paper we will take Cr(CO)₆ as the prototype system. The ligand-field splitting in the d manifold gives rise to e_g* orbitals, which are σ-antibonding between the metal d_g orbital and a lone pair on the ligand, as illustrated for the d_{z²} component in the figure. Excitation to the e_g* orbital reduces the number of electrons in the π-bonding t_{2g} orbitals and, more importantly, occupies the strongly antibonding Cr–d_{z²}–CO–5σ e_g* orbital. It is therefore understandable that the corresponding excited state potential energy curve (PEC) along the metal–CO dissociation coordinate is dissociative, the heterolytic dissociation leading to CO in the ground state and Cr(CO)₅ in the “t_{2g}” → “d_{z²}” excited state. The departure of the antibonding CO will lead to strong lowering of the orbital energy of the d_{z²}, the excitation energy therefore being much lower in Cr(CO)₅ than in Cr(CO)₆. This is also necessary since the energy available for the breaking of the Cr–CO bond is just the difference in excitation energy in the initial complex and in the photoproduct.

The excitation spectrum of Cr(CO)₆ contains a low-energy low-intensity shoulder that was assigned a long time ago by

Beach and Gray² to the ligand field excited state ¹T_{1g} belonging to the t_{2g}⁵e_g¹ configuration. At higher energies the high-intensity charge-transfer bands occur, with a weak band in between that has been assigned to the ¹T_{2g}(t_{2g}⁵e_g¹) LF state. This assignment appeared to be confirmed by the original extended-Hückel² as well as more recent semiempirical INDO/S CI⁹ and *ab initio* RHF¹⁰ calculations. There was also little reason for revision of this assignment, since irradiation in the low-energy shoulder, presumably populating the lowest LF state, leads to photodissociation of CO, in perfect agreement with the expectations. The Cr–CO photodissociation has been the subject of a number of time-resolved spectroscopic investigations,^{11–20} which have established that the dissociation is fast (within 350 fs¹⁸) and have mainly been directed toward the understanding of the effect of the solvent on the photodissociation dynamics and the reaction processes (vibrational relaxation and solvation). The LF nature of the photoactive excited state has not been questioned.

However, we have recently found in several d⁶ TM complexes^{5,21,6} that the relation between the lowest excited state at equilibrium geometry and the photochemistry is less direct than assumed in the “standard model”. In particular, the LF excitation to a metal–CO antibonding e_g-type orbital was found

[†] Permanent address: Institut für Technische Elektrochemie, Technische Universität Wien, A-1060 Vienna.

[⊗] Abstract published in *Advance ACS Abstracts*, July 1, 1997.

- (1) Gray, H. B.; Beach, N. A. *J. Am. Chem. Soc.* **1963**, *85*, 2922.
- (2) Beach, N. A.; Gray, H. B. *J. Am. Chem. Soc.* **1968**, *90*, 5731.
- (3) Pierloot, K.; Tsokos, E.; Vanquickenborne, L. G. *J. Phys. Chem.* **1996**, *100*, 16545.
- (4) Rosa, A.; Ricciardi, G.; Baerends, E. J.; Stufkens, D. J. *Inorg. Chem.* **1995**, *34*, 3425.
- (5) Rosa, A.; Ricciardi, G.; Baerends, E. J.; Stufkens, D. J. *Inorg. Chem.* **1996**, *35*, 2886.
- (6) Wilms, M. P.; Baerends, E. J.; Rosa, A.; Stufkens, D. J. *Inorg. Chem.* **1997**, *36*, 1541.
- (7) Geoffroy, G. L.; Wrighton, M. S. *Organometallic Photochemistry*; Academic: New York, 1979.
- (8) Ferraudi, G. J. *Elements of Inorganic Photochemistry*; John Wiley & Sons: New York, 1988.

(9) Kotzian, M.; Rösch, N.; Schröder, H.; Zerner, M. C. *J. Am. Chem. Soc.* **1989**, *111*, 7687.

(10) Pierloot, K.; Verhulst, J.; Verbeke, P.; Vanquickenborne, L. G. *Inorg. Chem.* **1989**, *28*, 3059.

(11) Burdett, J. K.; Grzybowski, J. M.; Perutz, R. N.; Poliakov, M.; Turner, J. J.; Turner, R. F. *Inorg. Chem.* **1978**, *17*, 147.

(12) Gerrity, D. P.; Rothberg, L. J.; Vaida, V. J. *Phys. Chem.* **1983**, *87*, 2222.

(13) Kelly, J. M.; Long, C.; Bonneau, R. J. *Phys. Chem.* **1983**, *87*, 3344.

(14) Fletcher, T. R.; Rosenfeld, R. N. *J. Am. Chem. Soc.* **1985**, *107*, 2203.

(15) Simon, J. D.; Xie, X. J. *Phys. Chem.* **1986**, *90*, 6751.

(16) Seder, R. A.; Church, S. P.; Weitz, E. J. *J. Am. Chem. Soc.* **1986**, *108*, 4721.

(17) Wang, L.; Zhu, X.; Spears, K. G. *J. Am. Chem. Soc.* **1988**, *110*, 8695.

(18) Joly, A. G.; Nelson, K. A. *J. Phys. Chem.* **1989**, *93*, 2876.

(19) Lee, M.; Harris, C. B. *J. Am. Chem. Soc.* **1989**, *111*, 8963.

(20) Joly, A. G.; Nelson, K. A. *Chem. Phys.* **1991**, *152*, 69.

(21) Rosa, A.; Ricciardi, G.; Baerends, E. J.; Stufkens, D. J. *J. Phys. Chem.* **1996**, *100*, 15346.

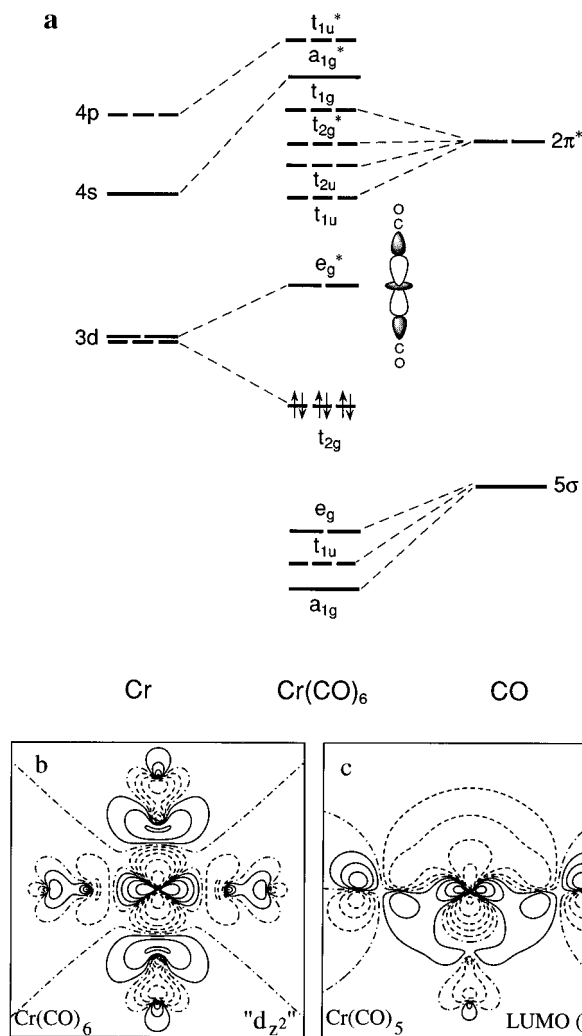


Figure 1. (a) Typical qualitative MO level diagram for a d⁶ metal carbonyl complex, as used to picture the LF splitting and rationalize the low-energy LF excitation and photoreactivity upon low-energy absorption. (b) Orbital contour plot of the virtual e_g^{*} ("d_{z²}") orbital of Cr(CO)₆. Contour values: ±0.5, ±0.2, ±0.1, ±0.05, ±0.02, and 0.0 [e/bohr]^{1/2}. (c) Orbital contour plot of the a₁ LUMO of Cr(CO)₅.

to lie at relatively high energy. On the other hand, the σ-antibonding character of such orbitals proved to be not only extremely strong but also short ranged. As a consequence, as soon as the metal–CO bond becomes longer, the pushing-up effect of the antibonding character rapidly diminishes, and the orbital energy and excitation energy come down precipitously. The initially high-lying LF state is therefore characterized by a very strongly dissociative PEC, which after fairly small metal–CO bond lengthening already leads to crossing with the PECs of the states that are lower lying at R_e. The implication is that photochemical metal–CO dissociation may take place regardless of the nature of the excited state into which the excitation takes place at equilibrium geometry. The photochemistry therefore does not give direct evidence for the nature of the excited state at R_e. In our examples the lowest excitation was to a σ-antibonding orbital between the metal and a ligand (L) other than CO (to L = Mn(CO)₅ in Mn₂(CO)₁₀,⁵ to Cl in MnCl(CO)₅,⁶ or to a π* orbital of an α-diimine ligand in *fac*-MnCl(CO)₃(α-diimine).²¹ In this last example the low-energy excitation is truly of the metal–ligand charge-transfer (MLCT) type.

It is improbable that the situation in the prototype Cr(CO)₆ system would be different. For this reason and because the system affords clear analysis of the electronic structure because of its high symmetry, we have been investigating the photo-

chemistry of this system. As before we use density functional (DF) calculations to obtain the PECs of the ground state as well as excited states. The DF calculations afford a straightforward interpretation of the electronic structure in terms of a molecular orbital picture. The DF calculations find, as in the other d⁶ complexes, the LF excitations to be at high energy at R_e, and not to be responsible for the photoactive low-energy weak-intensity transition. We have been encouraged by the very recent calculations by Pierloot et al.,¹⁰ who have performed CASPT2 calculations for the excited states of Cr(CO)₆. These calculations, which may be considered the most sophisticated ones to date, find, in agreement with our DF calculations and contrary to the previous calculations,^{9,10} the LF excited states to be at much higher energy than has been assumed before.

In the present paper we present a re-interpretation of the photochemistry of Cr(CO)₆ upon low-energy excitation (at ca. 4.0 eV), based upon calculated potential energy curves (PECs) along the Cr–CO dissociation coordinate. Our interpretation for Cr(CO)₆ is in line with the findings for the other d⁶ systems and leads to a reassessment of the role of LF excited states in the photochemistry. The calculated DF excitation energies at R_e, using the ΔSCF-type of approach originally suggested by Ziegler et al.²² (see below), will be compared to the recent CASPT2 results.

2. Method

All calculations have been performed with the Amsterdam Density Functional (ADF) program system.^{23–25} This computational scheme is characterized by a density fitting procedure²³ to obtain accurate Coulomb and exchange-correlation potentials and by evaluation of the KS hamiltonian matrix elements by an accurate and efficient 3D numerical integration method.^{26,24} An uncontracted double-ζ STO basis set has been used with one polarization function for the C and O atoms. For Cr a triple-ζ 3d,4s basis with one 4p function was used. The 1s O and C cores were kept frozen as well as the 1s–2p cores for Cr atom.

The density functionals included Becke's gradient correction²⁷ to the local exchange expression and Perdew's gradient correction²⁸ to the LDA expression (VWN²⁹ parametrization) for the correlation energy.

The original proof of the Hohenberg–Kohn theorem is only valid for the ground state of a system. It has been extended to the lowest state of any given symmetry, which is in fact sufficient for the purpose of this paper. However, the ΔSCF type method proposed by Ziegler *et al.*²² for the calculation of excited states has been used to obtain a number of higher excited states as well. This method has been used with good results for atomic^{30–32} and molecular systems,^{22,33–35} as well as the potential energy surface for the photodissociation of H₂O in its first excited state.³⁶ The results of the ΔSCF method are comparable to those of the theoretically better founded time-dependent DFT

(22) Ziegler, T.; Rauk, A.; Baerends, E. J. *Theor. Chim. Acta* **1977**, *43*, 261.

(23) Baerends, E. J.; Ellis, D. E.; Ros, P. *Chem. Phys.* **1973**, *2*, 41.

(24) te Velde, G.; Baerends, E. J. *J. Comput. Phys.* **1992**, *99*, 84.

(25) Fonseca Guerra, C.; Visser, O.; Snijders, J. G.; te Velde, G.; Baerends, E. J. Parallelisation of the Amsterdam Density Functional Program. In *Methods and Techniques for Computational Chemistry*; Clementi, E., Corongiu, G., Eds.; STEF: Cagliari, 1995; p 305.

(26) Boerrigter, P. M.; te Velde, G.; Baerends, E. J. *Int. J. Quantum Chem.* **1988**, *33*, 87.

(27) Becke, A. *Phys. Rev. A* **1988**, *38*, 3098.

(28) Perdew, J. P. *Phys. Rev. B* **1986**, *33*, 8822 (Erratum: **1986**, *34*, 7406).

(29) Vosko, S. H.; Wilk, L.; Nusair, M. *Can. J. Phys.* **1980**, *58*, 1200.

(30) von Barth, U. *Phys. Rev. A* **1979**, *20*, 1693.

(31) Wood, J. H. *J. Phys. B* **1980**, *13*, 1.

(32) Lannoo, M.; Baraff, G. A.; Schlüter, M. *Phys. Rev. B* **1981**, *24*, 943.

(33) Ziegler, T.; Rauk, A. *Theor. Chim. Acta* **1977**, *46*, 1.

(34) Rosa, A.; Baerends, E. J. *Inorg. Chem.* **1994**, *33*, 584.

(35) Daul, C.; Baerends, E. J.; Vernooijs, P. *Inorg. Chem.* **1994**, *33*, 3538.

(36) Doublet, M.-L.; Kroes, G. J.; Baerends, E. J.; Rosa, A. *J. Chem. Phys.* **1995**, *103*, 2538.

method^{37,38} with the adiabatic local-density approximation, which has recently been applied successfully to a number of simple atoms³⁹ and molecules.⁴⁰ The method for excitation energy calculation of ref 22 differs from a ΔSCF method as used in *ab initio* Hartree–Fock methods, where total energy differences are taken from possibly multideterminantal configuration state functions. A crucial element of the scheme of ref 22 is the restriction of total energy calculations to single-determinantal states only. This is a consequence of the requirements for the hole-density that have to be met for the approximate functionals to be applicable. It is, however, not always possible, particularly in a high point group symmetry, to resolve all multiplets of a given configuration from the energies of single determinants only, completely analogous to the situation in the traditional diagonal-sum method for multiplets.^{41,42} In those cases one may sometimes solve the problem by judicious symmetry lowering (e.g. to C_{4v} symmetry in our case, see below). More systematically, if one is prepared to go beyond diagonal-sum approaches and to calculate explicitly specific two-electron integrals,⁴³ any multiplet problem may be solved, where the maximum number of non-redundant two-electron integrals may be deduced by group-theoretical methods as developed by Daul.⁴⁴

We wish to stress that Kohn–Sham molecular orbitals are not just mathematical constructs whose only purpose is to build the electron density, they are physically meaningful (see ref 45 and references therein), in the same way as the MOs of other one-particle models such as Hartree–Fock and extended Hückel. This is related to the fact that the effective local potential of the Kohn–Sham model has as leading terms—apart from the nuclear potential and Coulomb potential of the total electronic density—the potential due to both the Fermi (exchange) hole and the Coulomb hole.^{46–48} The latter builds in effects of electronic correlation and in fact gives the Kohn–Sham MOs an advantage over Hartree–Fock orbitals in cases of strong near-degeneracy correlation. Virtual orbitals, being solutions in exactly the same potential as the occupied orbitals, have the advantage that they lack the artificial upshift and diffuse character of Hartree–Fock orbitals. They are useful for a qualitative interpretation of the electronic nature of excited states.

3. Results

In Table 1 the orbital energies of the 3d orbitals, the highest occupied orbital $2t_{2g}$ and the empty $6e_g$ orbital, are given, as well as those of the whole set of empty CO $2\pi^*$ orbitals and the Cr 4s orbital. We note that the $6e_g$ orbital is *not* the LUMO, as is assumed in the traditional MO scheme of Figure 1, but is actually quite high up in the virtual orbital spectrum. The spread in the CO $2\pi^*$ orbitals is substantial, amounting to more than 1.5 eV. It is caused by bonding and antibonding interactions between the CO molecules of the $(CO)_6$ cage. As a matter of fact, the spread is larger in the empty $(CO)_6$ cage since the

Table 1. One-Electron Energies and Percentage Composition (Based on Mulliken Population Analysis per MO) of $Cr(CO)_6$ MOs in Terms of Cr and CO Fragments

MO	ϵ (eV)	occ. ^a	Cr	CO
$9a_{1g}$	0.003	0	77 (5s), 23 (4s)	
$2t_{1g}$	-0.951	0		100 ($2\pi^*$)
$6e_g$	-1.127	0	61 ($3d_{z^2}$, $3d_{x^2-y^2}$)	39 (5σ)
$3t_{2g}$	-1.574	0	39 ($3d_{xy}$, $3d_{xz}$, $3d_{yz}$)	61 ($2\pi^*$)
$2t_{2u}$	-2.165	0		100 ($2\pi^*$)
$9t_{1u}$	-2.593	0	6 ($4p_x$, $4p_y$, $4p_z$)	7 (5σ), 88 ($2\pi^*$)
$2t_{2g}$	-6.591	6	59 ($3d_{xy}$, $3d_{xz}$, $3d_{yz}$)	41 ($2\pi^*$)

^a Orbital occupancy.

Table 2. Excitation Energies (eV) to the Charge-Transfer States Arising from the $(2t_{2g})^5(9t_{1u})^1$ and $(2t_{2g})^5(2t_{2u})^1$ Configurations, and to the Ligand-Field States Arising from the $(2t_{2g})^5(6e_g)^1$ Configuration with a Comparison Made to the CASSCF and CASPT2 Calculations of Pierloot *et al.*²

state	DFT	CASSCF ^a	CASPT2 ^a	expt ^b
CT excited states				
$a^1T_{2u}(2t_{2g} \rightarrow 9t_{1u})$	4.0	5.18–5.26	3.70–3.56	
$a^1E_u(2t_{2g} \rightarrow 9t_{1u})$	4.0	5.11–5.28	3.41–3.59	
$a^1A_{2u}(2t_{2g} \rightarrow 9t_{1u})$	4.2	5.14–5.32	3.58–3.58	
$b^1E_u(2t_{2g} \rightarrow 2t_{2u})$	4.5	5.86–6.16	3.97–4.05	
$a^1A_{1u}(2t_{2g} \rightarrow 2t_{2u})$	4.5	5.92–6.29	4.15–4.10	
$b^1T_{2u}(2t_{2g} \rightarrow 2t_{2u})$	5.0	6.21–6.57	4.32–4.43	
$a^1T_{1u}(2t_{2g} \rightarrow 9t_{1u})$	5.6	6.15–5.97	4.54–4.11	4.43
$b^1T_{1u}(2t_{2g} \rightarrow 2t_{2u})$	6.5	7.16–7.75	5.07–5.20	5.41
LF excited states				
$^1T_{1g}(2t_{2g} \rightarrow 6e_g)$	5.2	5.66	4.85	
$^1T_{2g}(2t_{2g} \rightarrow 6e_g)$	6.3	6.42	5.08	

^a The energy range indicated for the CASSCF and CASPT2 results refers to different choices of active spaces, see ref 2 for details. ^b From ref 1.

lowest one in the cage is the mostly strongly CO–CO bonding t_{2g} combination of $2\pi^*$ orbitals, which in the complex is shifted up considerably by the π -antibonding with the $3d-t_{2g}$ orbitals. The σ -antibonding present in the $6e_g$ is however so strong that it puts the $6e_g$ orbital (nominally 3d) even higher, close to the top of the $2\pi^*$ band (in a Hartree–Fock calculation we found the same picture, with actually the $6e_g$ even above the whole $2\pi^*$ band). The σ -antibonding between d_{z^2} and the C lone pair on CO is clearly visible in Figure 1b. We also note that the mixing between the 3d orbitals and the CO orbitals is strong in both the π bond (the $2t_{2g}/3t_{2g}$ bonding/antibonding set) and the σ bond ($5e_g/6e_g$). The $6e_g$ is nominally a 3d orbital and the $3t_{2g}$ is nominally a $2\pi^*$ orbital, but both have ca. 40% admixture of other orbitals.

The orbital energies suggest that the LF states will not be the lowest states in the excitation spectrum. As shown in Table 2, we do indeed find that the lowest excited states have CT character. These are the a^1T_{2u} , a^1E_u , and a^1A_{2u} states that arise from $2t_{2g} \rightarrow 9t_{1u}$ orbital excitation (we will restrict ourselves to the singlet states at this point). The same configuration also leads to the much higher lying a^1T_{1u} state. Qualitatively the same picture is obtained in the CASSCF and CASPT2 calculations. At the CASSCF level the transition energies are quite high, typically 1–1.5 eV higher than our excitation energies. Adding the second order perturbation effects in the CASPT2 step leads to strong lowering, to the effect that the CASPT2 results are lower than our excitation energies, often in the order of 0.5 eV and sometimes more. We do come to the same ordering of the excited states, however. In particular, we both find the excited states above the low-lying a^1T_{2u} , a^1E_u , a^1A_{2u} set to be the b^1E_u , b^1A_{1u} , b^1T_{2u} set of states arising from the next CT transition, the $2t_{2g} \rightarrow 2t_{2u}$ orbital excitation. Again the fourth state belonging to this excited configuration, b^1T_{1u} , is at much higher energy. The excitations from the ground state

(37) Runge, E.; Gross, E. K. U. *Phys. Rev. Lett.* **1984**, *52*, 997.

(38) Gross, E. K. U.; Kohn, W. *Adv. Quantum Chem.* **1990**, *21*, 255.

(39) Petersilka, M.; Gross, E. K. U. *Int. J. Quantum Chem. Symp.* **1996**, *30*, 181.

(40) Jamorski, C.; Casida, M.; Salahub, D. R. *J. Chem. Phys.* **1996**, *104*, 5134.

(41) Eyring, H.; Walter, J.; Kimball, G. E. *Quantum Chemistry*; J. Wiley & Sons: New York, 1944.

(42) Slater, J. C. *Quantum Theory of Atomic Structure*; McGraw-Hill: New York, 1960; Vol. 1.

(43) Dickson, R. M.; Ziegler, T. *Int. J. Quantum Chem.* **1996**, *58*, 681.

(44) Daul, C. *Int. J. Quantum Chem.* **1994**, *52*, 867.

(45) Baerends, E. J.; Gritsenko, O. V.; van Leeuwen, R. The effective one-electron potential in the Kohn–Sham molecular orbital theory. In *Chemical Applications of Density Functional Theory*; Laird, B. B., Ross, R. B., Ziegler, T., Eds.; American Chemical Society: Washington, DC, 1996; Vol. 629, p 20.

(46) Gritsenko, O. V.; van Leeuwen, R.; Baerends, E. J. *J. Chem. Phys.* **1994**, *101*, 8955.

(47) Süle, P.; Gritsenko, O. V.; Nagy, A.; Baerends, E. J. *J. Chem. Phys.* **1995**, *103*, 10085.

(48) Baerends, E. J.; Gritsenko, O. V.; van Leeuwen, R. Electron correlation and the structure of the exchange-correlation potential and the correlation energy density in density functional theory. In *New Methods in Quantum Theory*; Tsipis, C. A., Popov, V. S., Herschbach, D. R., Avery, J. A., Eds.; Kluwer Academic: Dordrecht, 1996; Vol. 8, p 395.

to a^1T_{1u} and b^1T_{1u} are the only ones allowed by both spin and spatial symmetry, cf. the discussions by Beach and Gray² and Pierloot et al.³ The crucial point for our discussion is that the lowest excitations are calculated to be the a^1T_{2u} , a^1E_u , a^1A_{2u} and b^1E_u , b^1A_{1u} , b^1T_{2u} sets of symmetry forbidden charge transfer excitations, both in the DFT and the CASSCF/CASPT2 calculations. These CT excitations are below the LF excitations. With respect to the LF states originating from the $(2t_{2g})^5(6e_g)^1$ configuration, we observe that the DFT results are again, as for the CT excitations, in between the CASSCF and the CASPT2 results. We have given in Table 2 all excited states that we find up to 5.2 eV, at which energy we encounter the lowest LF state. At higher energies the states arising from the other CT configurations $(2t_{2g})^5(3t_{2g})^1$ and $(2t_{2g})^5(2t_{1g})^1$ are found, some of which are located below the a^1T_{1u} and b^1T_{1u} states of the $(2t_{2g})^5(9t_{1u})^1$ and $(2t_{2g})^5(2t_{2u})^1$ configurations, but since we obtain basically the same pattern we refer to ref 3 for a discussion of the complete excitation spectrum to the CO $2\pi^*$ orbitals.

We conclude that our present DFT results for Cr(CO)₆ are in line with those for other d⁶ complexes^{4,21,6} and with the completely independent CASSCF/CASPT2 results. They strongly indicate that the LF excited states are too high to be directly populated when irradiation at ca. 4.0 eV takes place. The low intensity of the absorption at this energy is to be attributed to their symmetry-forbidden nature, not to their LF character. This poses the question how one can explain the observed photochemical metal–CO dissociation at this energy, and in particular what the role of the CT states that are being populated could be in the photochemical process.

We have calculated the PECs along the Cr–CO dissociation coordinate for the states arising from the $2t_{2g} \rightarrow 9t_{1u}$ CT excitation. Since the optimized geometry of the Cr(CO)₅ product does not differ much from the geometry of the Cr(CO)₅ fragment in Cr(CO)₆ (cf. discussions in refs 49 and 50), we have kept the geometry of the Cr(CO)₅ fragment fixed. The curves as shown in Figure 2 demonstrate that there are, in spite of the CT character of these states, two dissociative or nearly dissociative PECs, of 1B_2 and 1E symmetry in the relevant C_{4v} point group, arising from the a^1T_{2u} and a^1E_u states. The corresponding triplet states (Figure 2b) are both purely dissociative. This demonstrates that it is not necessary to excite to LF states in order to induce photodissociation of ligands, but that the dissociation may also occur from CT states. The observed photoactivity may therefore not be used for assigning the low-energy absorption to LF excitation. It should also be noted that the singlet PECs are dissociative, so that it is not necessary to invoke intersystem crossing to the dissociative triplet PECs in order to explain the photodissociation. In agreement with this, Joly and Nelson²⁰ concluded from their transient absorption measurements that the photodissociation proceeds directly from the initially excited state with no intersystem crossing necessary.

It is possible to understand from the electronic structure why this excitation is photoactive, and one can indeed predict immediately that precisely these B₂ and E PECs will be the dissociative ones. The essential element in the explanation is that, even though the excitation is to a CT state at R_e, the dissociation is still driven by the presence of a strongly dissociative LF state, which is at high energy at R_e but rapidly lowers its energy upon CO bond lengthening. The symmetry of the dissociative LF state, which can be predicted without calculation, then dictates B₂ and E symmetry for the dissociative PECs in Figure 2, as will become apparent below.

(49) Rosa, A.; Ehlers, A. W.; Baerends, E. J.; Snijders, J. G.; te Velde, G. *J. Phys. Chem.* **1996**, *100*, 5690.

(50) Folga, E.; Ziegler, T. *J. Am. Chem. Soc.* **1993**, *115*, 5169.

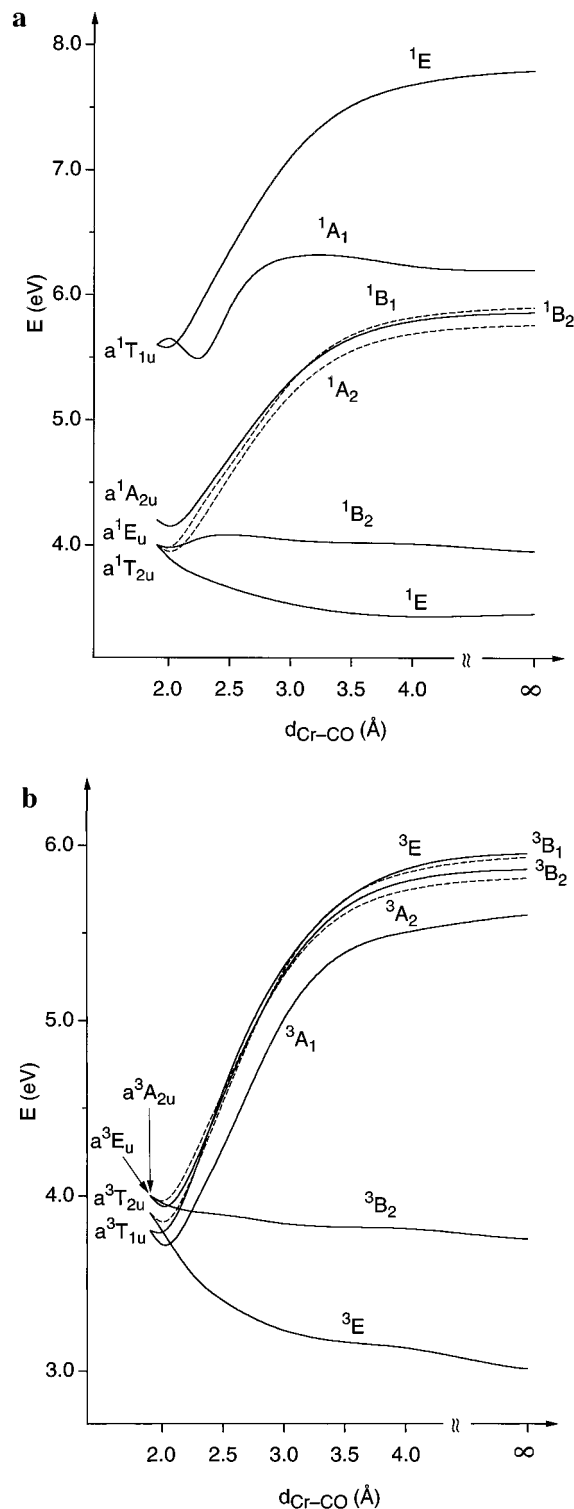
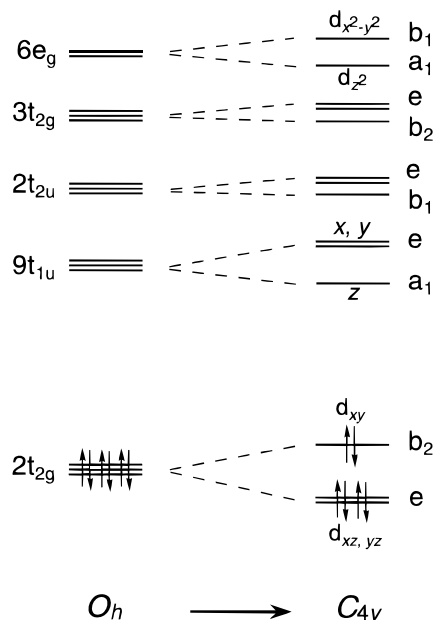


Figure 2. (a) Potential energy curves (PECs) along the Cr–CO dissociation coordinate for the singlet states (in C_{4v} symmetry) arising from the lowest excited (charge-transfer) configuration, $(2t_{2g})^5(9t_{1u})^1$. (b) The same for the corresponding triplet states.

The mechanism for the photodissociation is in fact *mutatis mutandis*, the same as that found in the other d⁶ complexes.^{4,21,6} Upon Cr–CO bond lengthening, the antibonding present in the Cr–d_{z²}–CO–5σ e_g^{*} orbital (we will denote it as “d_{z²}”, see Figure 1b) rapidly diminishes. When there is a ligand *trans* to the leaving CO with a weaker ligand field strength, such as Cl or Mn(CO)₅, the “d_{z²}” orbital precipitously lowers its energy. It will cross with the lower lying virtual levels, or exhibit an avoided crossing in the case of equal symmetry, and may ultimately become the lowest virtual orbital. This implies that

Scheme 1



the LF state corresponding to the excitation to “ d_z^2 ” starts at high energy but is strongly dissociative and may eventually become the lowest excited state. Whether the LF state actually crosses the CT excited state and becomes the lowest excited state in the metal fragment resulting from CO dissociation of course depends on the magnitude of the CT excitation energy. We have found²¹ that if an equatorial α -diimine ligand is present with a very low lying virtual π^* orbital, so that the CT excited state is at low energy, the lowering of the LF state is not sufficient to cross the low-lying CT state. Even in that case, CO dissociation may occur, but by a totally different mechanism, involving significant rearrangement of the metal fragment. However, in the systems $\text{Mn}(\text{CO})_5\text{-L}$ ($\text{L} = \text{Cl}$ or $\text{Mn}(\text{CO})_5$) the LF state does become the lowest excited state upon dissociation of the axial CO *trans* to L. In these cases, the symmetry of the LF state resulting from excitation to “ d_z^2 ” is equal to the symmetry of the lowest excited state at R_e (in the lower symmetry corresponding to the dissociating system). Since the LF state comes down, an avoided crossing between these states will occur along the dissociation coordinate. The first excited state PEC then either exhibits the typical barrier resulting from an avoided crossing, having the electronic structure of a LF excitation only *after* the barrier, or may be purely dissociative without a discernable barrier, the electronic structure in this state changing more gradually to the LF type. We have observed little tendency to formation of a barrier in the lowest excited state PECs for axial CO dissociation (none in triplet curves, very slight if at all in singlet curves). The state symmetry of the dissociative PECs is of course determined by the symmetries of the orbitals involved in the excitation, i.e. the highest occupied orbitals and the virtual dissociative “ d_z^2 ” orbital.

The situation in $\text{Cr}(\text{CO})_6$ appears to be very much analogous to the axial CO dissociation in the $\text{Mn}(\text{CO})_5\text{-L}$ cases, the present $^1\text{B}_2$ and ^1E PECs that originate from CT states have the same characteristics as we encountered before: no (^1E) or a small ($^1\text{B}_2$) barrier in the singlet curves, none in the triplet curves. However, the presence of the remaining *trans* CO ligand, with high ligand field strength, gives some modifications compared to the investigated cases with weaker axial ligands L, which makes the picture of a simple (avoided) crossing between the dissociative LF state and the CT state slightly

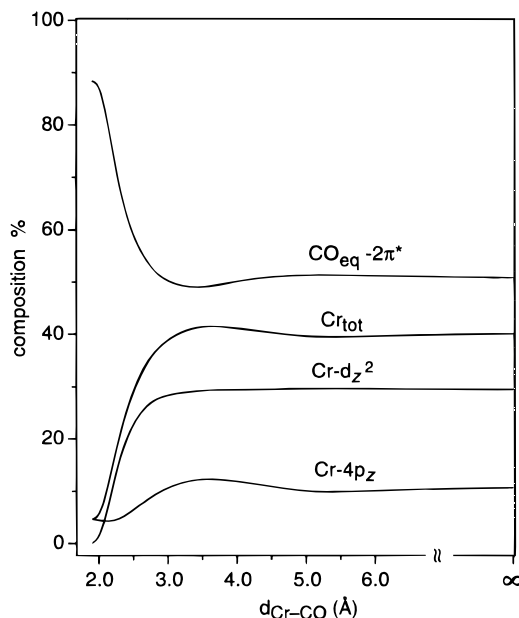


Figure 3. Changes in the composition of the lowest virtual orbital of $\text{Cr}(\text{CO})_6$ along the Cr–CO dissociation coordinate. The orbital is initially the a_1 component (in C_{4v} symmetry) of the $9t_{1u}$ (in O_h) level and evolves into the a_1 LUMO of $\text{Cr}(\text{CO})_5$. The percentage compositions are derived from a Mulliken population analysis.

oversimplified. Let us consider the splitting of the relevant orbitals upon lowering the symmetry from O_h to C_{4v} (Scheme 1).

The $\text{Cr-}d_z^2\text{-CO-}5\sigma$ e_g^* orbital has a_1 symmetry in C_{4v} , the same as one of the components of the $9t_{1u}$ orbitals. When an axial CO is moved away, this “ d_z^2 ” orbital will come down. We would expect this $a_1(6e_g)$ orbital to exhibit an avoided crossing with the $a_1(9t_{1u})$. This means that the states arising from the $2t_{2g} \rightarrow 9t_{1u}$ CT excitation, which have under the symmetry lowering become either $e(2t_{2g}) \rightarrow a_1(9t_{1u})$ or $b_2(2t_{2g}) \rightarrow a_1(9t_{1u})$, i.e. have E or B_2 symmetry in C_{4v} , will have an avoided crossing with E or B_2 LF states that have the electronic character $e(2t_{2g}) \rightarrow a_1(e_g)$ or $b_2(2t_{2g}) \rightarrow a_1(e_g)$. These latter LF states are strongly dissociative. The avoided crossing may result in a barrier on the PEC, but if the crossing is strongly avoided no barrier will appear. It is actually found completely lacking in ^1E in Figure 2 and to be weak in $^1\text{B}_2$. Indeed, in the calculations the orbital energies of the $a_1(6e_g)$ and the $a_1(9t_{1u})$ orbitals never come very close—the $a_1(6e_g)$ does come down in energy initially, but it does not get really close to the lower-lying $a_1(9t_{1u})$ since at larger Cr–CO bond distances (2.0 Å and beyond) the $a_1(9t_{1u})$ energy actually drops more quickly. So we do not have the simple picture that the $a_1(6e_g)$, characterized by significant d_z^2 character, on its way down crosses the $a_1(9t_{1u})$, which has zero d_z^2 character at R_e as well as at larger distances. The character of these orbitals changes in a somewhat more complicated way. Along the Cr–CO dissociation coordinate these two orbitals gradually but considerably mix, the symmetry lowering also giving rise to other orbital admixing, such as $4p_z$. Ultimately the LUMO of $\text{Cr}(\text{CO})_5$, which evolves smoothly from the $a_1(9t_{1u})$, has about as much d_z^2 character as the higher lying a_1 orbital, the latter however incorporating all of the antibonding with the axial CO that is left behind. We refer to ref 4 for a detailed discussion of these two a_1 orbitals in $\text{Mn}(\text{CO})_5$, which is very similar to $\text{Cr}(\text{CO})_5$, with a full account of the role of the remaining axial CO 5σ orbital, the $4p_z$ orbital, and the equatorial CO $2\pi^*$ orbitals. We show in Figure 3 how the composition of the initially lower a_1 orbital (starting as $a_1(9t_{1u})$) changes as a function of the Cr–CO distance. The building

up of Cr- d_{z^2} character in this orbital between 2.0 and 2.5 Å is clearly visible. In Cr(CO)₅ this orbital becomes the well-known $d_{z^2}-2\pi_{\text{eq}}-4p_z$ LUMO with high amplitude at the vacant site and good acceptor properties. The change in going from the $a_1(6e_g)$ (i.e. " d_{z^2} ") to the a_1 LUMO of Cr(CO)₅ can be appreciated by comparing the contour plots of these orbitals in Figure 1, parts b and c. The plot of the Cr(CO)₅ LUMO shows the strong mixing of equatorial CO 2π with Cr $4p_z$ and $3d_{z^2}$ in this orbital. In view of the hybrid nature of the a_1 LUMO of Cr(CO)₅ one cannot unequivocally denote excitation to this orbital either as LF or as CT excitation. Nevertheless, the picture that the Cr–CO dissociation from a state that has CT character at R_e can be understood from the (strongly avoided) crossing of this state by a strongly dissociative LF state captures the essence of the electronic structure explanation in the case of Cr(CO)₆ as well as in the Mn(CO)₅L cases.

It is clear now that among the states that arise from the $2t_{2g} \rightarrow 9t_{1u}$ excitation those that can be derived from orbital excitation to the a_1 component (in C_{4v} symmetry) of the $9t_{1u}$ will be the ones that can give rise to states with dissociative PECs, either with a barrier or barrierless. The $e(2t_{2g}) \rightarrow a_1(9t_{1u})$ and $b_2(2t_{2g}) \rightarrow a_1(9t_{1u})$ excitations give rise to E and B₂ states in C_{4v} , respectively. All the other states from the $(2t_{2g})^5(9t_{1u})^1$ configuration in O_h , corresponding to $e \rightarrow e$ excitation (A_1 , A_2 , B_1 , and B_2 states in C_{4v}) and $b_2 \rightarrow e$ excitation (E state in C_{4v}), are not expected to be dissociative. This is corroborated by the calculations of the PECs (see Figure 2). Most of the PECs (1A_2 , 1B_2 , 1B_1 , 1E) simply curve upward, the energy rising due to the loss of bonding to the leaving CO. It is interesting to observe that the 1A_1 state arising from the a^1T_{1u} behaves somewhat differently. This is due to the changes in the electronic structure of this state along the dissociation coordinate. Upon Cr–CO bond lengthening this 1A_1 state originates from an $e \rightarrow e$ excitation. The virtual e orbitals that at R_e belong to the antibonding CO- π^* -Cr- $3d_{\pi}$ $3t_{2g}$ set, drop in energy due to loss of this antibonding character. The e orbital to which the excitation takes place goes down in energy and acquires considerable $e(\pi^*-3d_{\pi})$ character. At longer bond lengths excitation to an orbital with much leaving CO π^* character implies an excited state with large charge separation (negative CO, positive Cr(CO)₅ fragment) and therefore corresponds to high energy. The 1A_1 PEC therefore goes up, but not very much since it experiences an avoided crossing with the first $e \rightarrow e$ 1A_1 excited state of the Cr(CO)₅ fragment. The asymptotic electronic character along this PEC is therefore this CT excitation in Cr(CO)₅.

4. Conclusions

We conclude that the role of LF excited states in the photochemistry of TM complexes may be somewhat different than has been generally assumed. We find, in agreement with previous calculations on this and other d^6 complexes with CO

ligands (both DFT^{4–6} and CASSCF/CASPT2³), that LF excitations are at relatively high energy at R_e . In the case of Cr(CO)₆ the low-energy shoulder in the spectrum has been attributed² to a LF excited state, which appeared to be in agreement with the low intensity as well as its leading to photolytic metal–CO bond cleavage. We find in agreement with Pierloot et al.³ that symmetry forbidden transitions to low-energy CT states should be responsible for the absorption in the low-energy regime (ca. 4.0 eV). Some of these CT states are calculated to be dissociative, accounting for the experimentally observed photoactivity. The mechanism that makes the states dissociative is in essence (see above for details) the rapid lowering upon Cr–CO bond lengthening of Cr–CO antibonding LF states that are high lying at R_e . The antibonding in the e_g^* orbital to which the excitation takes place in the LF excited states is strong, causing the high excitation energy, but it also appears to be rather short ranged, causing the orbital energy to drop rapidly upon bond lengthening. This lowering of the orbital energy has been apparent in previously investigated cases where the ligand field strength of the nondissociating *trans* ligand was relatively weak. In Cr(CO)₆ the remaining axial CO causes the dissociation to proceed without a clear (avoided) crossing of one-electron levels, but the rapid loss of antibonding between d_{z^2} and the leaving CO causes considerable d_{z^2} character to revert from the high-lying e_g^* to the lowest virtual orbital, while in the process the orbital energy of this orbital becomes lower, as does the energy of the states (E and B₂) resulting from excitation from the HOMO $2t_{2g}$ into this orbital. This makes the PECs of these states dissociative.

We have found the lowest Cr $\rightarrow 2\pi^*$ MLCT excited state, as well as various other types of lowest excited state that had very little or no metal–CO antibonding character, to be photoactive with respect to metal–CO dissociation. This demonstrates that it is not necessary to excite to LF states in order to induce photodissociation of ligands, and that such dissociation, when observed, does not prove that the excitation was to a LF state. However, the accepted picture that metal–ligand dissociation occurs from LF excited states is based on an underlying assumption, namely, that LF states are dissociative, which is fully corroborated by the calculations: they actually are so strongly dissociative that even if they are too high to be populated directly by irradiation into the lowest absorption band, they cross so soon with the lowest excited states that the lowest excited state PEC becomes dissociative.

Acknowledgement. We wish to thank Prof. D. J. Stufkens of the University of Amsterdam for exciting our interest in the photochemistry of metal–ligand bonds and for many suggestions and discussions. C.P. acknowledges support as an Erasmus exchange student in the project ICP-95-A-3008/13 (Prof. K. Schwarz, Vienna, coordinator).

JA970592U